Chemistry of Metals and Alloys

Chem. Met. Alloys 11 (2018) 6-13
Ivan Franko National University of Lviv
www.chemetal-journal.org

The ternary systems Al–Ga–Pd and Ga–Sb–Pd. Search for new catalytic materials

Oksana MATSELKO[1,2]*, Ulrich BURKHARDT[2], Yuri GRIN[2], Roman GLADYSHEVSKII[1]

[1] *Department of Inorganic Chemistry, Ivan Franko National University of Lviv, Kyryla i Mefodiya St. 6, 79005 Lviv, Ukraine*
[2] *Max-Planck-Institut für Chemische Physik fester Stoffe, Nöthnitzer Straße 40, 01187 Dresden, Germany*
* *Corresponding author. Tel.:* +380-32-2394506*; e-mail: oksana.matselko@lnu.edu.ua*

Received April 25, 2018; accepted June 27, 2018; available on-line September 3, 2018

The phase relations in the Pd-rich region (≥ 50 at.% Pd) of the ternary systems Al–Ga–Pd at 600°C and Ga–Sb–Pd at 500°C have been investigated by means of X-ray powder diffraction and EDX analysis. Four continuous substitutional solid solutions were found in the Al–Ga–Pd system: $Al_{1-x}Ga_xPd$ (FeSi-type structure, space group *P*2_13, Pearson symbol *cP*8), $(Al_{1-x}Ga_x)_3Pd_5$ (Rh_5Ge_3-type structure, space group *Pbam*, Pearson symbol *oP*16), $Al_{1-x}Ga_xPd_2$ (Co_2Si-type structure, space group *Pnma*, Pearson symbol *oP*12), $(Al_{1-x}Ga_x)_2Pd_5$ (Pd_5Ga_2-type structure, space group *Pnma*, Pearson symbol *oP*28). In the Pd-rich part of the Ga–Sb–Pd system, three new ternary phases were revealed: $Ga_{1-x}Sb_xPd_2$ (Fe_2P-type structure, space group *P*-62*m*, Pearson symbol *hP*9) and two tetragonal phases with approximate compositions close to $Ga_{0.5}Sb_{0.5}Pd_3$, one of which crystallizes with Pt_3Ga-type structure (space group *P*4/*mbm*, Pearson symbol *tP*16). The existence of the previously reported phase $Ga_{4.5}Sb_{4.5}Pd_{25}$ was confirmed. The isothermal sections were constructed for the Pd-rich regions of both systems. The catalytic properties of the sample $Ga_{28.3}Sb_5Pd_{66.7}$ were investigated for semi-hydrogenation of acetylene.

Aluminum / Gallium / Antimony / Palladium / Isothermal section / Phase diagram / Semi-hydrogenation of acetylene

Introduction

The catalytic properties of Ga–Pd intermetallic compounds [1] and recent investigations of Ga–Sn–Pd phases [2,3] make the ternary systems of gallium with metals/semimetals of the groups 13-15 of the periodic table (*M*) and platinum metals (*T*) attractive for the search for new catalytic materials.

The systems Ga–*M*–*T* have not been thoroughly investigated (Table 1, [4]). Of the 66 ternary systems Ga–*M*–*T*, isothermal sections of the phase diagrams (mainly partial; calculated or experimental) have been constructed only for 10: Ga–As–Rh [5-7], Ga–{Si,Ge,As,Sb}–Pd [5,8-11], Ga–As–{Os,Ir} [5,12], and Ga–{Ge,As,Sb}–Pt [5,13-18] (Table 2). 14 ternary compounds, representing 11 structure types, have been reported in the following systems: Ga–{Ge,As}–Rh [10,19], Ga–{Si,Ge,As,Sb,Bi}–Pd [3,8-10,20,21], Ga–B–{Ir,Pt} [22,23], and Ga–Ge–Pt [13] (Table 3). It should be noted that almost all of the known compounds are rich in platinum metal (~60-80 at.% *T*). Only 5 structure types are fully ordered, while all the others contain sites with mixed occupancies of Ga and the other *p*-element. In addition, the structures of the ternary compounds in these systems are characterized by longer distances between the platinum metal atoms than in elemental *T* (Fig. 1, [24]). According to the active-site isolation concept [25], isostructural intermetallic compounds may be interesting as potential, not only active, but selective, catalytic materials, for example, for the semi-hydrogenation of acetylene.

Here, we present the phase relations in the Pd-rich region (≥ 50 at.% Pd) of the ternary systems Al–Ga–Pd and Ga–Sb–Pd at 600°C and 500°C, respectively.

Experimental

Alloys of the systems Al–Ga–Pd, Ga–Sb–Pd were synthesized from elemental aluminum (rods, AlfaAesar, 99.9965 mass%), gallium (pellets,

ChemPur, 99.9999 mass%), antimony (shots, ChemPur, 99.999 mass%), and palladium (granules, ChemPur, 99.95 mass%), by arc melting under argon atmosphere (Ti-getter, water-cooled copper hearth, tungsten electrode) in a glove box filled with argon (O_2 and H_2O content ≤ 1 ppm). After the arc melting, the ingots were annealed at 600°C in molybdenum containers made from foil, or in glassy carbon crucibles (samples with Al), or at 500°C in alumina crucibles (samples with Sb) in evacuated quartz tubes for two months, followed by quenching in water. In order to check particular regions of the isothermal sections several samples were chosen in each system and annealed for six months at the appropriate temperature.

Characterization was performed by means of room-temperature X-ray powder diffraction (XRPD) on Image plate Guinier camera (Huber G670, Cu $K\alpha_1$), *in situ* temperature dependent XRPD (STOE Stadi MP in Debye-Scherrer geometry, Cu $K\alpha_1$), scanning electron microscopy (SEM) (Philips XL30, LaB_6 cathode) with energy dispersive X-ray spectroscopy (EDXS) (Bruker EDX-Quantax, SD-Detector DE(Mn $K\alpha$) = 123 eV), and wavelength dispersive X-ray spectroscopy (WDXS) (CAMECA SX100) on metallographic cross-sections. For the XRPD analysis all Pd-rich samples (> 70 at.% Pd), due to their high mechanical strength and ductility, were filed and reannealed for 24 h.

Catalytic measurements were performed in a stainless steel reactor (inner diameter 9.14 mm) with a quartz glass frit to support the catalyst bed for the semi-hydrogenation of acetylene. A powdered sample (grain size 20-32 μm) was mixed with 420 mg catalytically inert BN (Alfa Aesar, hexagonal, 99.5 mass%, 325 mesh) to improve the flow characteristics of the reactants and the heat distribution in the catalyst bed. A total flow of 40 mL·min^{-1}, consisting of 0.5 vol.% C_2H_2, 5 vol.% H_2, 50 vol.% C_2H_4 was used for isothermal (200°C) measurements. The gases were mixed using mass flow controllers (Bronkhorst). The gas phase composition was analyzed by a gas chromatograph (Varian Micro GC CP4900) with three different columns (molecular sieve, Al_2O_3, and polydimethylsiloxane).

Table 1 Level of investigation of the Ga–*M*–*T* systems: phase diagrams (grey) and compounds (black).

	M											*T*
	B	Al	In	Tl	Si	Ge	Sn	Pb	As	Sb	Bi	
Ga												Ru
												Rh
												Pd
												Os
												Ir
												Pt

Table 2 Phase diagram studies of ternary systems Ga–*M*–*T*.

System	Investigation	Temperature	Concentration range	Reference
Ga–As–Rh	calculated	25°C	complete	[5,6]
	experimental	1000°C	complete	[6]
	experimental	800°C	complete	[7]
Ga–Si–Pd	experimental	600°C	0-70 at.% Si; 0-70 at.% Pd	[8]
Ga–Ge–Pd	experimental	700°C	50-100 at.% Pd	[9]
Ga–As–Pd	calculated	25°C	complete	[5]
	experimental	600°C	0-66.7 at.% Pd	[8]
	experimental	1000°C	0-66.7 at.% Pd	[10]
Ga–Sb–Pd	experimental	500°C	0-50 at.% Pd	[11]
Ga–As–Os	calculated	25°C	complete	[5]
Ga–As–Ir	calculated	25°C	complete	[5]
	experimental	600°C	complete	[12]
Ga–Ge–Pt	experimental	700°C; 800°C	0-80 at.% Pt	[13]
Ga–As–Pt	calculated	25°C	complete	[5,14,15]
	calculated	600°C	complete	[15]
	calculated	400°C	complete	[15]
	experimental	600°C	complete	[16]
Ga–Sb–Pt	experimental	500°C	complete	[17,18]

Table 3 Crystallographic parameters of ternary Ga–*M*–*T* compounds (grey: fully ordered structures).

No.	Compound	Structure type	Pearson symbol	Space group	Cell parameters			Reference
					a, Å	*b*, Å	*c*, Å	
1	$Ga_{0.2}Ge_{0.8}Rh$	FeSi	*cP*8	$P2_13$	4.832	–	–	[19]
2	Ga_2AsRh_5	La_2SnS_5	*oP*16	*Pbam*	5.463	10.215	4.019	[10]
3	$Ga_3Si_4Pd_{12}$	Th_7S_{12}	*hP*20	$P6_3/m$	9.377	–	3.619	[8]
4	$Ga_2Ge_5Pd_{12}$	Th_7S_{12}	*hP*20	$P6_3/m$	9.448	–	3.684	[9]
5	$Ga_{4.5}As_{2.5}Pd_{12}$	Th_7S_{12}	*hP*20	$P6_3/m$	9.425	–	3.708	[8]
6	$GaAsPd_5$	Pd_5TlAs	*tP*7	*P*4/*mmm*	3.949	–	6.876	[20]
7	$Ga_{4.5}As_{4.5}Pd_{25}$	$Pd_{25}Ge_9$	*hP*34	*P*-3	7.368	–	10.603	[21]
8	$Ga_{4.5}Sb_{4.5}Pd_{25}$	$Pd_{25}Ge_9$	*hP*34	*P*-3	7.500	–	10.732	[21]
9	$Ga_{0.5}Bi_{0.5}Pd_3$	Cu_3Au	*cP*4	*Pm*-3*m*	3.968	–	–	[20]
10	Ga_8BIr_4	Ir_4Ga_8B	*tI*104	$I4_1/acd$	8.5369	–	21.0569	[22]
11	$Ga_{2.7}B_5Ir_9$	$Pt_9Zn_3B_4$	*hP*17	*P*-62*m*	9.0465	–	2.8703	[23]
12	$Ga_3B_4Pt_9$	$Pt_9Ga_3B_4$	*hP*32	*P*-62*c*	8.7503	–	6.3742	[23]
13	$Ga_{0.75}Ge_{0.25}Pt_2$	Co_2Si	*oP*12	*Pnma*	5.523	4.057	7.900	[13]
14	$Ga_{0.6}Ge_{0.4}Pt_3$	U_3Si	*tI*16	*I*4/*mcm*	5.498	–	7.878	[13]

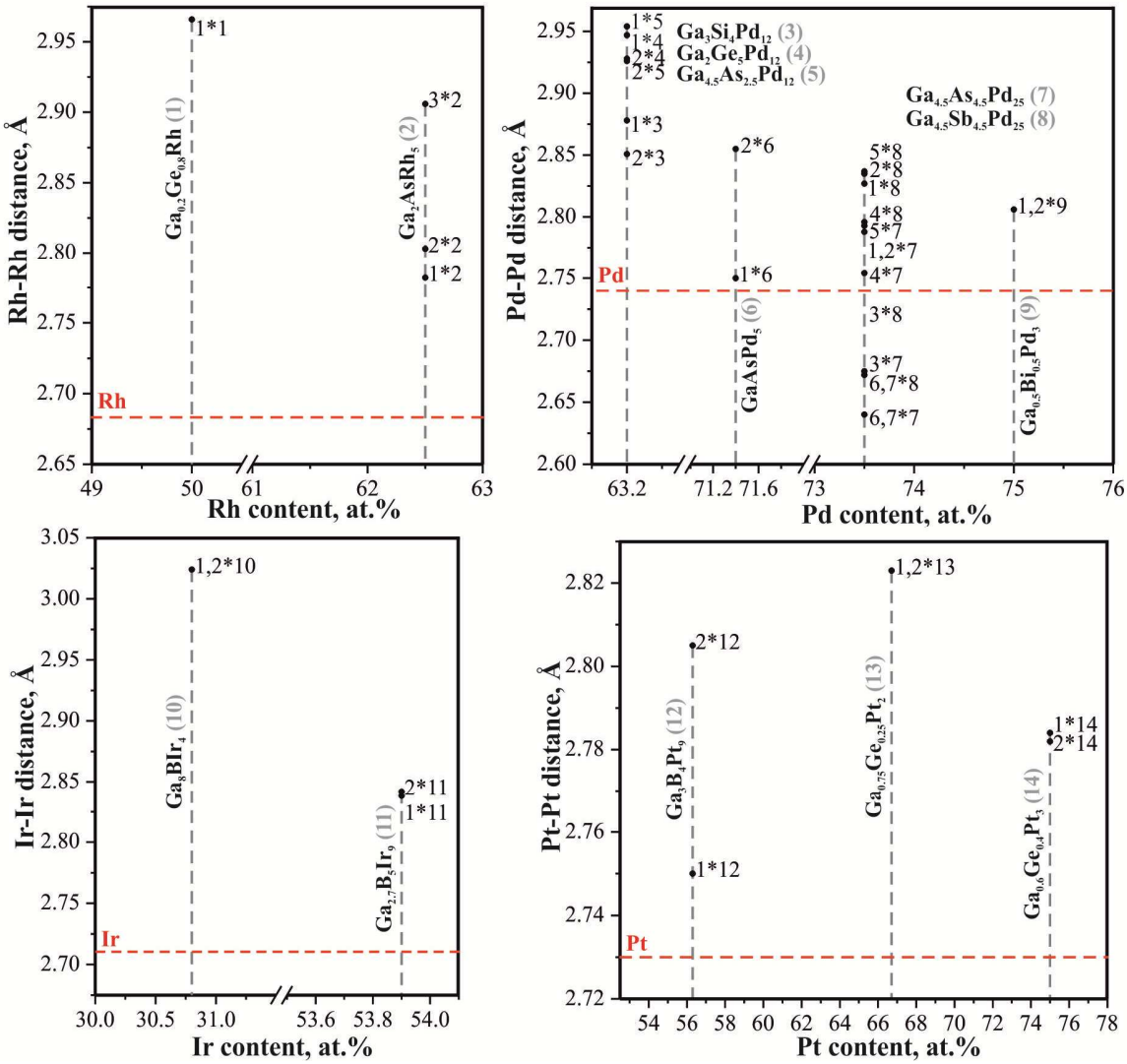

Fig. 1 Distances between platinum metal atoms in the crystal structures of ternary Ga–*M*–*T* compounds (for example, **1**,**2***10 means: the shortest *T*-*T* distance for the sites *T***1** and *T***2** for the compound #**10** in Table 3).

Results and discussion

In the Al–Ga–Pd and Ga–Sb–Pd ternary systems we expect the formation of solid solutions based on the binary compounds and, taking into account the diversity of the structure types adopted by Ga–*M*–*T* intermetallic compounds, new ternary compounds with unique crystal structures and, thus, properties.

The boundary binary systems, Al–Pd, Ga–Pd, Sb–Pd, Al–Ga, Ga–Sb, are well investigated. Assessed phase diagrams of the {Al,Ga,Sb}–Pd systems have been published by Okamoto [26-28], Al–Ga by Murray [29], and Ga–Sb by Ngai *et al.* [30]. The systems Al–Ga and Ga–Sb are quite simple, while the {Ga,Al,Sb}–Pd systems show a relatively complex character of the interaction of the components, especially in the Pd-rich regions [31]. Consequently, the phase relations in the system Al–Ga–Pd are expected to be complex, too.

Ternary system Al–Ga–Pd

The isothermal section of the Al–Ga–Pd system was constructed at 600°C in the range ≥ 50 at.% Pd (Fig. 2).

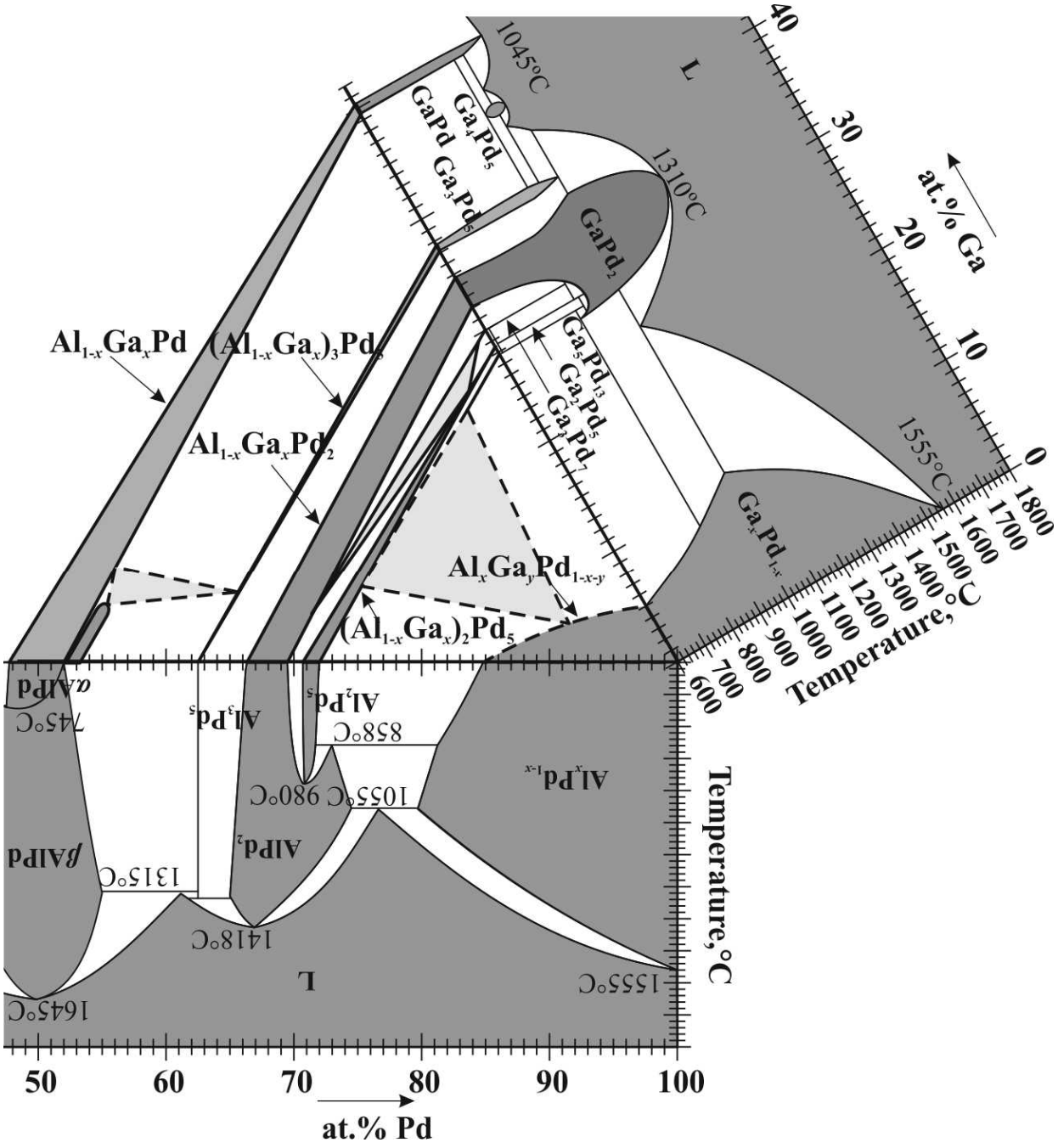

Fig. 2 Isothermal section of the phase diagram of the system Al–Ga–Pd at 600°C and ≥ 50 at.% Pd (together with the phase diagrams of the boundary binary systems Al–Pd and Ga–Pd, redrawn from [26,27]).

Four continuous substitutional solid solutions between isostructural compounds were found: $Al_{1-x}Ga_xPd$ (FeSi-type structure, |space group $P2_13$, Pearson symbol *cP*8), $(Al_{1-x}Ga_x)_3Pd_5$ (Rh_5Ge_3-type structure, space group *Pbam*, Pearson symbol *oP*16), $Al_{1-x}Ga_xPd_2$ (Co_2Si-type structure, space group *Pnma*, Pearson symbol *oP*12), $(Al_{1-x}Ga_x)_2Pd_5$ (Pd_5Ga_2-type structure, space group *Pnma*, Pearson symbol *oP*28) with $0 \le x \le 1$. Solid solutions based on two modifications of ~AlPd were observed. The structure of the second phase was found to be trigonal, in disagreement with the assessed binary Al–Pd phase diagram presented in [26], which shows two cubic modifications.

Ternary system Ga–Sb–Pd

The system Ga–Sb–Pd had already been investigated. A partial isothermal section (≤ 50 at.% Pd) at 500°C was constructed by Richter and Ipser [11] and the existence of one ternary phase, $Ga_{4.5}Sb_{4.5}Pd_{25}$ ($Pd_{25}Ge_9$-type structure, space grop *P*-3, Pearson symbol *hP*34), was reported by Ellner and El-Boragy [21].

Samples in the system Ga–Sb–Pd were prepared in the whole concentration range. The results confirmed the existence of the $Ga_{4.5}Sb_{4.5}Pd_{25}$ phase and the previously determined partial isothermal section.

All the binary phases, except Ga_3Pd_5, show significant solubility of the third component at a constant concentration of Pd at 500°C (the highest solubility, up to 8 at.% Sb, was found for $GaPd_2$). Three new ternary phases were revealed in the Pd-rich part of the phase diagram: $Ga_{1-x}Sb_xPd_2$ with x = 0.5-0.7 (Fe_2P-type structure, space group *P*-62*m*, Pearson symbol *hP*9) [32] and two tetragonal phases with primitive unit cells and approximate compositions close to $Ga_{0.5}Sb_{0.5}Pd_3$, one of which crystallizes in a Pt_3Ga-type structure (space group *P*4/*mbm*, Pearson symbol *tP*16) [33]. According to an *in situ* temperature-dependent XRPD study (25-750°C) on as cast samples, the tetragonal phase with Pt_3Ga-type structure exists till 600°C, whereas the other phase is stable till 700°C (Fig. 3). At higher temperatures (samples *a* and *b*) a cubic phase forms. The ternary phase $Ga_{4.5}Sb_{4.5}Pd_{25}$ was found to be stable, at least, up to 750°C.

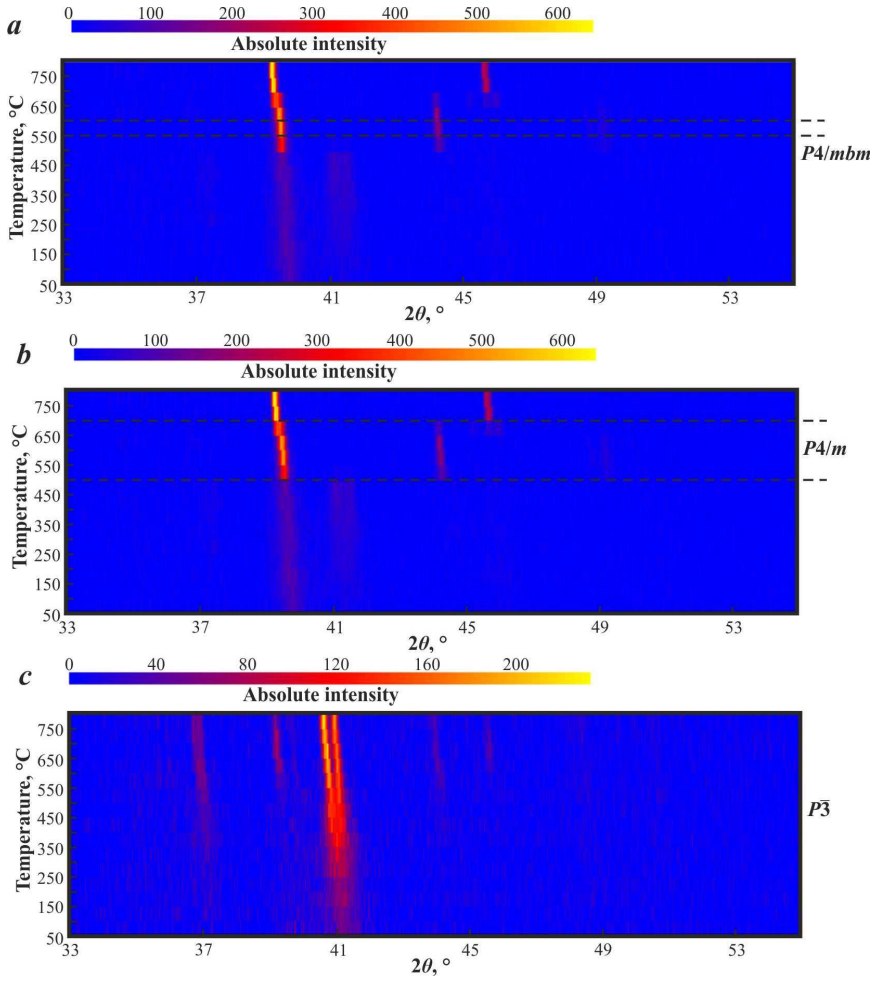

Fig. 3 Temperature ranges of the existence of the Pd-rich phases in the Ga-Sb-Pd system: powder patterns of the samples $Ga_{12.6}Sb_{10.3}Pd_{77.1}$ (*a*), $Ga_{12.5}Sb_{12}Pd_{75.5}$ (*b*), and $Ga_{10}Sb_{16}Pd_{74}$ (*c*).

After cooling from 750°C to room temperature we found only the tetragonal phase with the Pt_3Ga-type structure, whereas both tetragonal phases were observed after cooling from 550°C. Compositions of the Pd-rich phases according to the WDXS analysis are: $Ga_{14.6(1)}Sb_{10.8(1)}Pd_{74.6(1)}$ (*P*4/*mbm*), $Ga_{14.2(8)}Sb_{9.6(2)}Pd_{76.2(9)}$ (*P*4/*m*), and $Ga_{11.9(1)}Sb_{15.1(1)}Pd_{73.0(1)}$ (*P*-3). The phase relations in the Pd-rich region (≥ 50 at.% Pd) are presented in Fig. 4.

Catalytic properties

Taking into account the properties of $GaPd_2$ [1] and $Ga_{1-x}Sn_xPd_2$ [2], the solid solution $Ga_{1-x}Sb_xPd_2$ (sample with nominal composition $Ga_{28.3}Sb_5Pd_{66.7}$) was chosen to test its catalytic properties in the semi-hydrogenation of acetylene.

An investigation of the catalytic properties of unsupported $Ga_{1-x}Sb_xPd_2$ for acetylene semi-hydrogenation was conducted with an excess of ethylene.

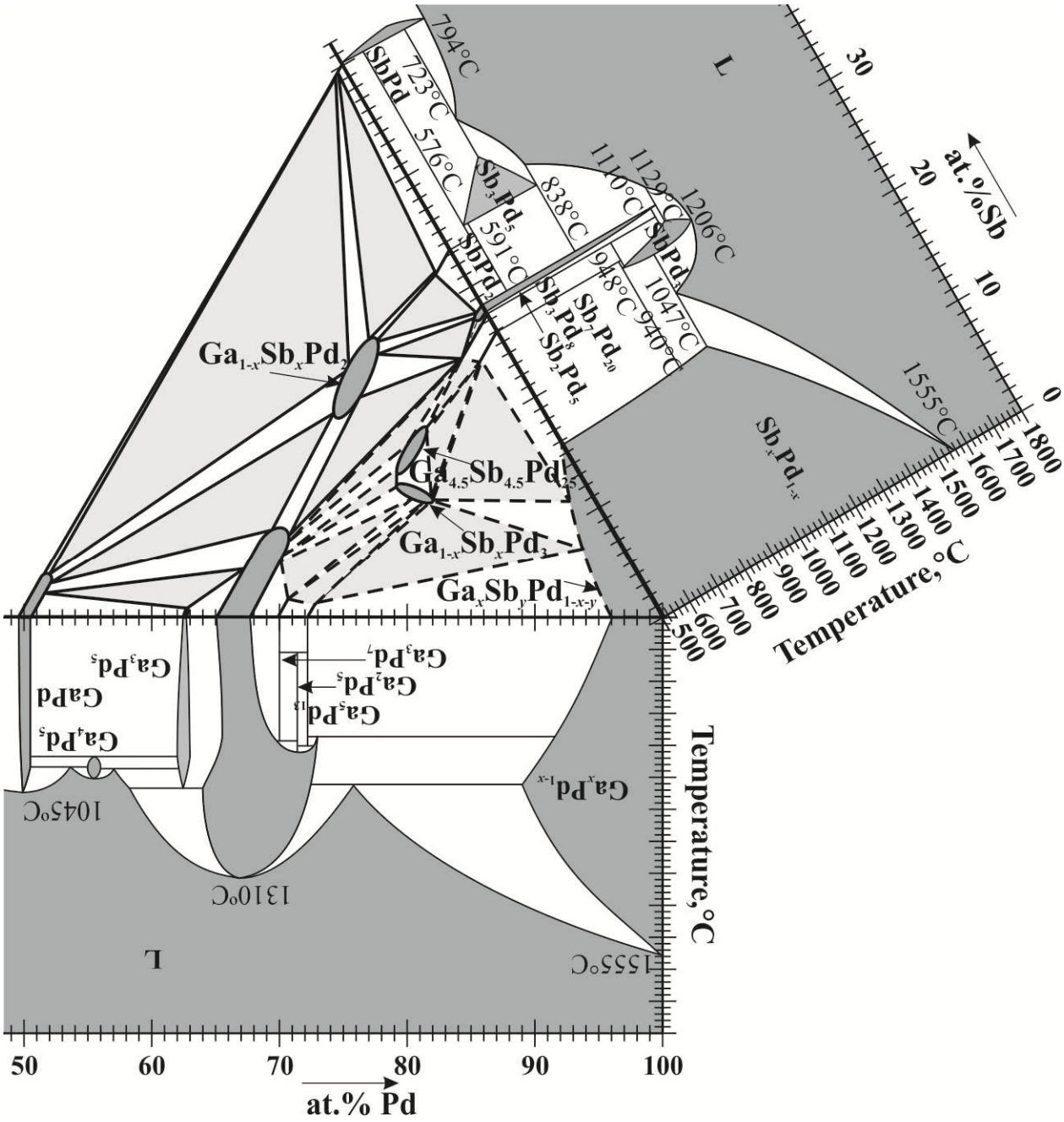

Fig. 4 Isothermal section of the phase diagram of the system Ga–Sb–Pd at 500°C and ≥ 50 at.% Pd (together with the phase diagrams of the boundary binary systems Ga–Pd and Sb–Pd, redrawn from [27,28]).

An isothermal catalytic experiment was carried out by heating the investigated alloy (6.23 mg, diluted with 420 mg BN) in helium to a reaction temperature of 200°C, followed by switching to ethylene-rich feed. Very high acetylene conversion (approaching 100 %) and high selectivity towards ethylene (75 %) were observed (Fig. 5). In addition, the observed activity is comparable with the most active sample of the solid solution $Ga_{1-x}Sn_xPd_2$ [2]. These findings correlate with the geometric and electronic models for semi-hydrogenation of acetylene [34].

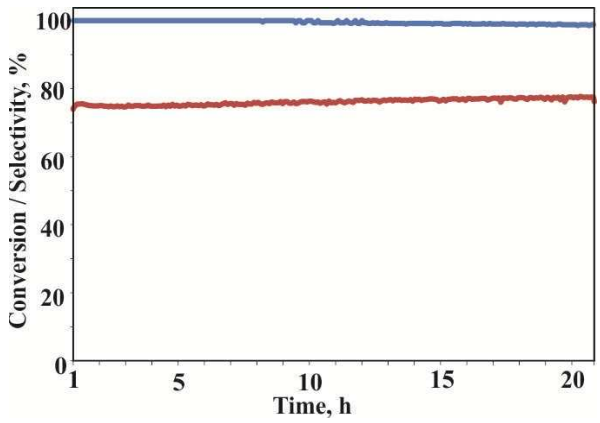

Fig. 5 Catalytic behavior – conversion of acetylene (blue) and selectivity to ethylene (red) – of the sample with nominal composition $Ga_{28.3}Sb_5Pd_{66.7}$ during semi-hydrogenation of acetylene.

Conclusions

The phase relations in the ternary systems Al–Ga–Pd and Ga–Sb–Pd are relatively complex. Nevertheless, the revealed phases (solid solutions and ternary compounds), especially of the Ga–Sb–Pd system, may be used as model catalysts in the semi-hydrogenation of acetylene. Despite the very high activity of $Ga_{28.3}Sb_5Pd_{66.7}$, the corresponding solid solution requires further investigation.

Acknowledgements

The authors are grateful to P. Scheppan, M. Eckert, and S. Kostmann for help during the metallographic investigations; Yu. Prots, H. Borrmann, R. Cardoso-Gil, and S. Hückmann for the XRPD experiments; M. Armbrüster and R.R. Zimmermann for the catalytic properties measurements, and I. Veremchuk for technical suggestions.

References

[1] M. Armbrüster, K. Kovnir, M. Behrens, D. Teschner, Yu. Grin, R. Schlögl, *J. Am. Chem. Soc.* 132 (2010) 14745-14747.
[2] O. Matselko, R.R. Zimmermann, A. Ormeci, U. Burkhardt, R. Gladyshevskii, Yu. Grin, M. Armbrüster, *J. Phys. Chem. C.*
[3] O. Matselko, U. Burkhardt, Yu. Prots, R.R. Zimmermann, M. Armbrüster, R. Gladyshevskii, Yu. Grin, *Eur. J. Inorg. Chem.* 29 (2017) 3542-3550.
[4] SpringerMaterials (*https://materials.springer.com*).
[5] R. Schmid-Fetzer, *J. Electron. Mater.* 17 (1988) 193-200.
[6] R. Guérin, A. Guivarc'h, Y. Ballini, M. Secoué, *Rev. Phys. Appl.* 25 (1990) 411-422.
[7] K.J. Schulz, O.A. Musbah, Y.A. Chang, *J. Phase Equilib.* 12 (1991) 10-14.
[8] M. El-Boragy, K. Schubert, *Z. Metallkd.* 72 (1981) 279-282.
[9] S. Heinrich, K. Schubert, *Z. Metallkd.* 66 (1975) 353-355.
[10] S. Députier, J.Y. Pivan, R. Guérin, *J. Less-Common Met.* 171 (1991) 357-368.
[11] K.W. Richter, H. Ipser, *Ber. Bunsenges. Phys. Chem.* 102 (1998) 1245-1251.
[12] K.J. Schulz, O.A. Musbach, Y.A. Chang, *Bull. Alloy Phase Diagrams* 11 (1990) 211-215.
[13] T.K. Chattopadhyay, K. Khalaff, K. Schubert, *Metall (Berlin)* 28 (1974) 1160-1168.
[14] Y.K. Kim, D.A. Baugh, D.K. Shuh, R.S. Williams, *J. Mater. Res.* 5 (1990) 2139-2151.
[15] M. Li, C. Li, F. Wang, W. Zhang, *J. Alloys Compd.* 437 (2007) 71-79.
[16] X.-Y. Zheng, K.J. Schulz, J.-C. Lin, Y.A. Chang, *J. Less-Common Met.* 146 (1989) 233-239.
[17] S.L. Markovski, M.C.L.P. Pleumeekers, A.A. Kodentsov, F.J.J. van Loo, *J. Alloys Compd.* 268 (1998) 188-192.
[18] K.W. Richter, H. Ipser, *J. Alloys Compd.* 281 (1998) 241-248.
[19] P. Eßlinger, K. Schubert, *Z. Metallkd.* 48 (1957) 126-134.
[20] M. El-Boragy, K. Schubert, *Z. Metallkd.* 61 (1970) 579-584.
[21] M. Ellner, M. El-Boragy, *J. Less-Common Met.* 161 (1990) 147-158.
[22] W. Klünter, W. Jung, *Z. Anorg. Allg. Chem.* 621 (1995) 197-200.
[23] K. Petry, W. Klünter, W. Jung, *Z. Kristallogr.* 209 (1994) 151-156.
[24] P. Villars, K. Cenzual (Eds.), *Pearson's Crystal Data. Crystal Structure Database for Inorganic Compounds*, Release 2016/17, ASM International, Materials Park (OH), 2016.
[25] W.M.H. Sachtler, *Catal. Rev.: Sci. Eng.* 14 (1976) 193-210.

[26] H. Okamoto, *J. Phase Equilib. Diffus.* 35 (2014) 105-116.
[27] H. Okamoto, *J. Phase Equilib. Diffus.* 29 (2008) 466-467.
[28] H. Okamoto, *J. Phase Equilib*. 13 (1992) 578-579.
[29] J.L. Murray, *Bull. Alloy Phase Diagrams* 4 (1983) 183-190.
[30] T.L. Ngai, R.C. Sharma, Y.A. Chang, *Bull. Alloy Phase Diagrams* 9 (1988) 586-591.
[31] P. Villars, K. Cenzual, J.L.C. Daams, F. Hulliger, T.B. Massalski, H. Okamoto, K. Osaki, A. Prince, S. Iwata, *Pauling File. Inorganic Materials Database and Design System. Binaries Edition*, Crystal Impact, Bonn, 2001.
[32] O. Matselko, U. Burkhardt, Yu. Grin, R. Gladyshevskii, *Z. Kristallogr. – New Cryst. Struct.* 233 (2018) 89-90.
[33] O. Matselko, U. Burkhardt, R. Gladyshevskii, Yu. Grin, *Z. Kristallogr. – New Cryst. Struct.* 233 (2018) 87-88.
[34] M. Armbrüster, In: I.T. Horvath (Ed.), *Encyclopedia of Catalysis*, Online Edition, Wiley, 2011.